Geophysical Research Letters

RESEARCH LETTER
10.1029/2023GL104954

Little Change in Apparent Hydrological Sensitivity at Large CO_2 Forcing

Dana Raiter[1,2], Lorenzo M. Polvani[1,2,3], Ivan Mitevski[3], Angeline G. Pendergrass[4,5], and Clara Orbe[3,6]

[1]Department of Earth and Environmental Sciences, Columbia University, New York, NY, USA, [2]Lamont-Doherty Earth Observatory, Columbia University, Palisades, NY, USA, [3]Department of Applied Physics and Applied Mathematics, Columbia University, New York, NY, USA, [4]Department of Earth and Atmospheric Sciences, Cornell University, Ithaca, NY, USA, [5]Climate and Global Dynamics Laboratory, National Center for Atmospheric Research, Boulder, CO, USA, [6]NASA Goddard Institute for Space Studies, New York, NY, USA

Key Points:

- We examine the dependence of apparent hydrological sensitivity (η_a, defined as $\Delta P/\Delta T$) on the magnitude of CO_2 forcing
- We find little change in η_a in abrupt 2× to 8×CO_2 experiments and a transient 1%/year experiment up to 8×CO_2
- Little change in η_a, notably at large CO_2, is also found in most CMIP5, CMIP6, and Longrun-MIP models

Supporting Information:

Supporting Information may be found in the online version of this article.

Correspondence to:

D. Raiter,
dana.raiter@columbia.edu

Citation:

Raiter, D., Polvani, L. M., Mitevski, I., Pendergrass, A. G., & Orbe, C. (2023). Little change in apparent hydrological sensitivity at large CO_2 forcing. *Geophysical Research Letters*, *50*, e2023GL104954. https://doi.org/10.1029/2023GL104954

Received 15 JUN 2023
Accepted 4 SEP 2023

Abstract Apparent hydrological sensitivity (η_a), the change in the global mean precipitation per degree K of global surface warming, is a key aspect of the climate system's response to increasing CO_2 forcing. To determine whether η_a depends on the forcing amplitude we analyze idealized experiments over a broad range of abrupt CO_2 forcing, from 2× to 8× preindustrial values, with two distinct climate models. We find little change in η_a between 2× and 4×CO_2, and almost no change beyond 5×CO_2. We validate this finding under transient CO_2 forcing at 1%-per-year, up to 8×CO_2. We further corroborate this result by analyzing the 1%-per-year output of more than 15 CMIP5/6 models. Lastly, we examine the 1,000-year long LongrunMIP model output, and again find little change in η_a. This wealth of results demonstrates that η_a is a very weak function of CO_2 forcing.

Plain Language Summary Hydrological sensitivity (HS) is defined as the change in globally-averaged precipitation per degree K of surface temperature increase caused by increasing concentrations of greenhouse gasses, such as CO_2. It is important to understand how HS changes with different levels of CO_2 in the atmosphere. To do this we analyzed model experiments with varying increases of CO_2. We find little change in HS between 2× to 4× the pre-industrial levels of CO_2, and almost no change beyond 5×CO_2. Additionally, we analyze model experiments where CO_2 concentrations increase by 1% per year and see similar results. Finally, we validate this finding with models with significantly longer run times. We thus conclude that HS is independent of the level of CO_2 in the atmosphere.

1. Introduction

Equilibrium Climate Sensitivity (ECS) is the global mean change in surface temperature for a doubling of CO_2 from the pre-industrial (PI) value. ECS is one of the key metrics used in assessing future global warming, and therefore plays a very important role in climate change related policy-making. One important question in this regard is how ECS changes in a warmer world. Several studies found that ECS increases at higher CO_2 concentrations (e.g., Bloch-Johnson et al., 2021; Colman & McAvaney, 2009; Gregory et al., 2015; Meraner et al., 2013). And, more recently, Mitevski et al. (2021) found a non-linear and non-monotonic dependence of ECS on CO_2 concentrations.

In addition to the surface temperature response, the precipitation response is another critical aspect of climate change. To evaluate precipitation changes, the key metric used is Hydrological Sensitivity (HS). HS is defined as the difference in global mean precipitation per one degree of global mean temperature change from the PI control state. Previous studies have explored the response of the hydrological cycle to global warming by examining HS in terms of the global energy budget, and have described the mechanisms affecting it (e.g., Allen & Ingram, 2002; Held & Soden, 2006; Jeevanjee & Romps, 2018; O'Gorman et al., 2011). The fact that HS is energetically constrained means that the precipitation response can be separated into fast and slow components. The fast response depends only on the CO_2 concentrations in the atmosphere, before the surface temperature has time to warm, and results in a decrease in precipitation. The slow response, in contrast, is associated with surface warming, and results in an increase in precipitation (Andrews et al., 2010).

One might ask if ECS and HS are related. Watanabe et al. (2018) suggested an anti-correlation between ECS and HS due to the low cloud response in a warmer world. More recently, however, Pendergrass (2020) revisited this connection using Phase 6 of the Coupled Model Intercomparison Project (CMIP6, Eyring et al. (2016)) and found no correlation between ECS and HS. Nonetheless, since ECS was found to be strongly affected by the magnitude of CO_2 forcing, one might ask if HS, as another aspect of the climate response, could also be affected in the same way, even if ECS and HS are not related.

We are aware of only one study which explored this subject (Good et al., 2012), which reported that HS decreases at higher CO_2 concentrations. However, that finding was obtained with a single climate model. Furthermore, the range of CO_2 forcing explored in that study was limited, as the authors only considered three values of CO_2 (0.5×, 2×, and 4×CO_2). Whether the finding of Good et al. (2012) can be confirmed with different climate models and over a broader range of CO_2, remains to be determined.

The goal of our study, therefore, is to answer this question. We do this by using two fully-coupled models, analyzing the changes in HS under abrupt CO_2 forcing, ranging from 2× to 8×CO_2. We also study changes in HS under the more realistic transient 1%/year CO_2 forcing scenario, with both models, and additionally in over 15 CMIP5 and CMIP6 models. And, finally, we examine HS under abrupt 2×, 4×, and 8×CO_2 in several LongrunMIP models, each run for 1,000 years. In all these, we find little change in HS with increased CO_2 forcing, especially under the stronger forcing cases.

2. Methods

We analyze output from the fully-coupled atmosphere-ocean-sea-ice-land model versions of the Community Earth System Model (CESM-LE, Hurrell et al. (2013)) and the NASA Goddard Institute for Space Studies ModelE (GISS E2.1-G, Kelley et al. (2020)). We use output that was previously analyzed by Mitevski et al. (2021) which performed a series of abrupt CO_2 forcing runs, with 2×, 3×, 4×, 5×, 6×, 7×, and 8×CO_2 with respect to the PI value, with all other natural and anthropogenic forcings fixed at PI values. Each run is 150 years long, as per the CMIP standard prescription for abrupt4xCO2 runs. We also analyze transient 1%/yr (1pctCO2) experiments for both CESM-LE and GISS E2.1-G from 1× to 8×CO_2 previously performed by Mitevski et al. (2021).

In addition to these two models, we also analyze output from both CMIP5 (Taylor et al., 2012) and CMIP6 (Eyring et al., 2016) models forced under the 1pctCO2 scenario. The list of models used can be found in Tables S2 and S3 in Supporting Information S1. Furthermore, we analyze five LongrunMIP models (Rugenstein et al., 2019): MPI-ESM1.2, HadCM3L, CCSM3, CESM1.0.4, and FAMOUS. For each of these models we analyze 1,000 years after the abrupt 2×, 4×, and 8×CO_2 increase (with the exception of FAMOUS, for which only the abrupt 2× and 4×CO_2 experiments were run to 1,000 years).

In all cases, we define global-averaged precipitation and surface temperature changes (ΔP and ΔT) as the difference from the PI control values. For the abrupt n×CO_2, following Fläschner et al. (2016), one can define the HS η as the slope of the linear regression of ΔP versus ΔT, that is,

$$\Delta P = \eta \Delta T + A \tag{1}$$

where A is the fast adjustment of the precipitation to CO_2 increase. However, since variables η and A, as defined in Equation 1, can only be calculated in abrupt increase in CO_2 experiments, we here prefer to use the apparent HS (this is referred to as endpoint η_a in Fläschner et al. (2016)); η_a is simply the ratio $\Delta P/\Delta T$. The advantage of η_a is that it can be calculated for both the transient and abrupt runs. For the abrupt runs, the ratio η_a is computed over the last 10 years of the model runs, following Fläschner et al. (2016); for the transient runs, η_a is just an instantaneous value. The quantities η and η_a are illustrated in Figure S1 in Supporting Information S1, which shows ΔP versus ΔT for the abrupt CO_2 forcing runs of the CESM-LE model.

3. Results

We start by examining how HS varies with CO_2 increase in the abrupt forcing experiments. Figure 1 shows the value of η_a for the fully-coupled CESM-LE runs (solid blue, values can be found in Table S1 in Supporting Information S1). One can see only small variations with CO_2 forcing, with the line becoming basically flat beyond 4×CO_2. This fact—which constitutes the key result of our paper—is corroborated by the runs performed with the

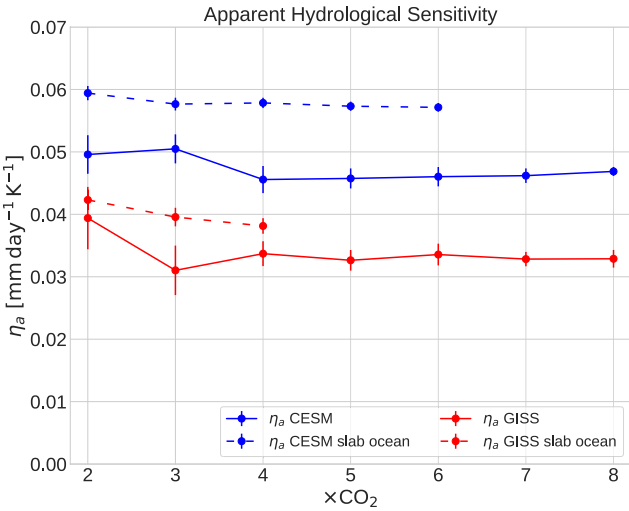

Figure 1. Apparent hydrological sensitivity, η_a calculated from fully coupled (solid lines) and slab ocean (dashed lines) CESM-LE (blue) and GISS E2.1-G (red) abrupt 2× to 8×CO_2 runs. Data is globally and annually averaged. Error bars denote 95% confidence intervals.

fully-coupled GISS E2.1-G model (solid red, Table S1 in Supporting Information S1). The lack of changes in HS at high CO_2 forcing is not dependent on the definition of HS. Using the second definition of HS, η in Equation 1, also reveals basically flat lines beyond 5×CO_2 (Figure S2a and Table S1 in Supporting Information S1). Note that the values of η_a are smaller than those of η, as the former includes the fast adjustment (Fläschner et al., 2016).

The reader might wonder about the small kink at 4×CO_2 in the CESM-LE runs, and 3×CO_2 in the GISS E2.1-G runs (Figure 1). To understand this behavior, we analyze additional experiments with identical forcings but with the slab-ocean configuration of both models where the ocean heat transport is fixed. We find that the kinks disappear in the slab-ocean runs (Figure 1, dashed lines), indicating that the non-monotonicity is due to changes in the ocean circulation. Mitevski et al. (2021) analyzed these runs in more detail and attributed the non-monotonic behavior to the formation of the North Atlantic Warming Hole caused by the collapse of the Atlantic Meridional Overturning Circulation (AMOC). The changes in η_a associated with AMOC collapse are relatively small for the CESM-LE model, less than 10%, and a little more substantial for the GISS E2.1-G model, ~20% (Figure 1). The key point, however, is that these changes disappear at larger CO_2 forcing.

In Figure S2b in Supporting Information S1 we show the fast adjustment A, calculated as the y-intercept of the regression of ΔP versus ΔT (see Equation 1), as a function of CO_2 forcing. A is the precipitation response before the surface temperature has had time to warm. The black line in Figure S2b in Supporting Information S1 is the linear regression of A versus the log of the CO_2 forcing. For both models we find that A is proportional to the log of the CO_2 concentration (with the exception of 4×CO_2 in CESM-LE and 3×CO_2 in GISS E2.1-G) as expected, considering that A is caused by the CO_2 radiative forcing, which is approximately a logarithmic function of its concentration.

Having obtained a robust result from the abrupt forcing experiments, we next explore the more realistic transient forcing experiments. In Figure 2 we show η_a in the transient 1pctCO2 experiments, for both models, with CO_2

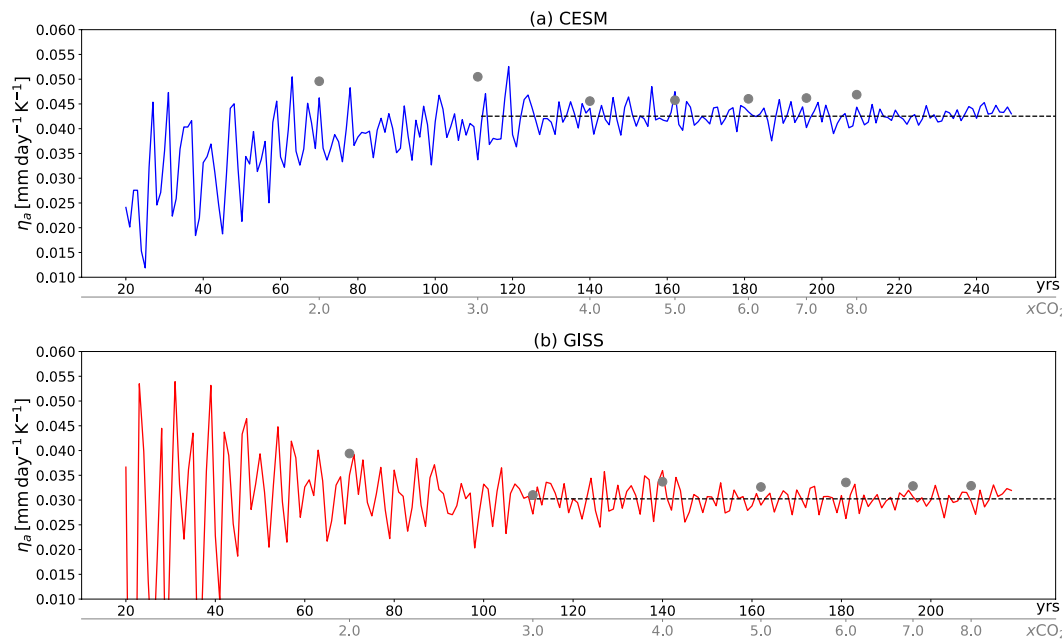

Figure 2. Time series of the apparent hydrological sensitivity, η_a, calculated from fully coupled 1pctCO2 CESM-LE (a, blue line) and GISS E2.1-G (b, red line) runs. Gray dots mark η_a calculated from the abrupt runs (Figure 1) and the dashed line marks the mean of 3–8×CO_2.

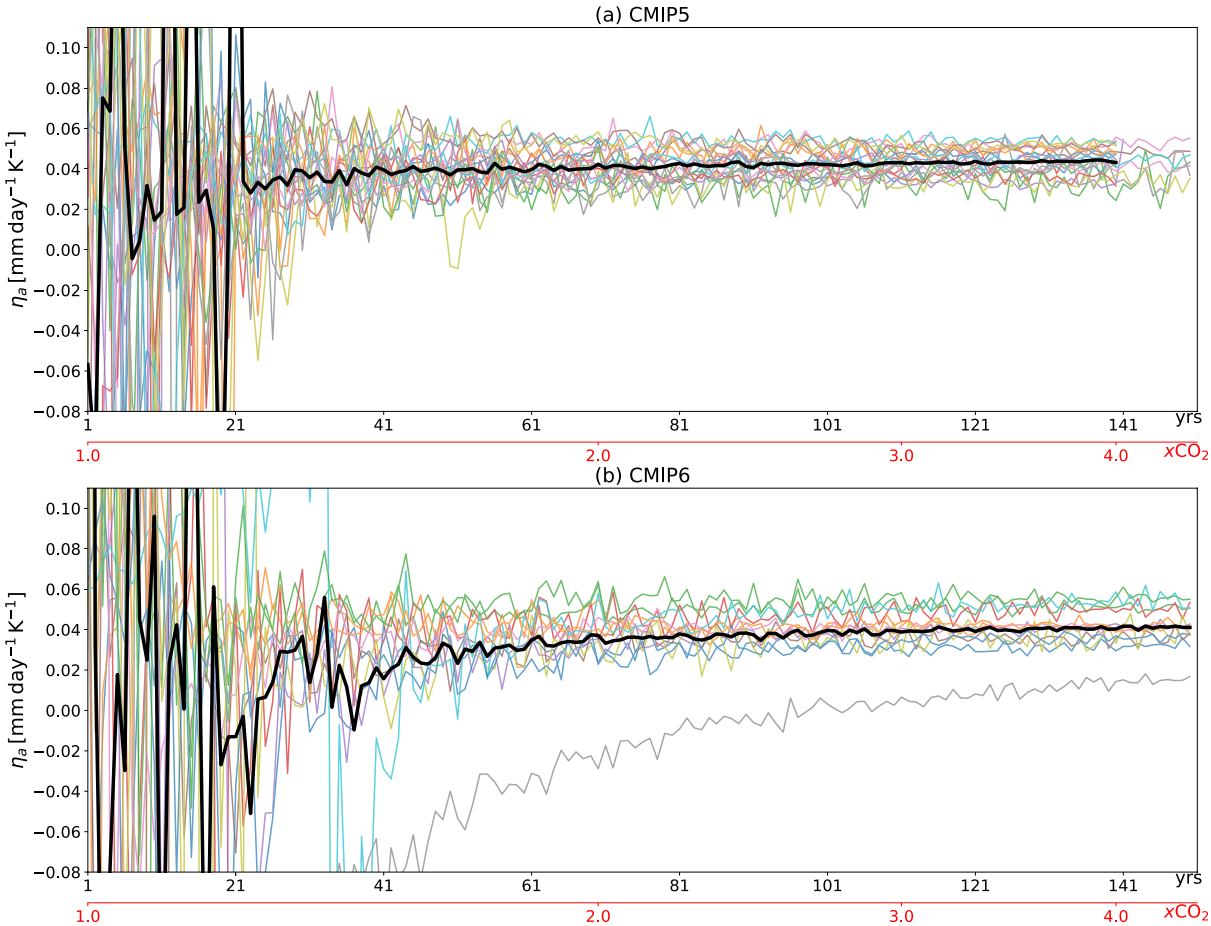

Figure 3. Time series of the apparent hydrological sensitivity, η_a, for CMIP5 and CMIP6 data, 1pctCO2 experiment (colored lines). Black line is the model mean.

ranging from PI to 8×CO_2 values. Beyond 3×CO_2, the value of η_a is constant (note that we have added an additional *x*-axis to show the CO_2 values over time). The gray dots in that figure show the values of η_a from the abrupt forcing experiments at the corresponding CO_2 value. The agreement between the abrupt and transient values of η_a corroborates our key finding, that HS is very nearly constant at large CO_2 forcing.

Next, we confirm that the lack of change in HS with CO_2 holds true over a larger set of climate models. We plot η_a in the 1pctCO2 scenario in 31 CMIP5 and 15 CMIP6 models, showing individual models in colored lines, and the multi-model mean in black, in Figure 3. Even though the CMIP models are run only up to 150 years and only up to 4×CO_2, we can see the flattening of the η_a line, so that HS becomes almost constant at the end of the models' run.

Finally, we address the question of time scales. Some might argue that, in the abrupt experiments, 150 years is not enough to reach an equilibrated state, and thus to obtain the full effect of the slow response on the hydrological cycle. To address this concern, we thus analyze all the LongrunMIP models for which 1,000 years are available (there are five such models, see Section 2). With solid lines in Figure 4 we show η_a, averaged over the last 10 years of the runs, calculated for these five models for the abrupt 2×, 4×, and 8×CO_2 experiments (note that the FAMOUS model lacks the abrupt8× data point). Similarly to the results shown above over the shorter 150 year period, we find very small changes in HS in these LongrunMIP models, with one outlier (HadCM3L). For that model, we note that η_a changes more than in the other four (by 31% from 2 to 8). However, its value of η_a lies well outside the range of the other four at 2×CO_2. Also, at 4×CO_2—where we have an additional 6 models available—that model is again the outlier. Leaving that model aside, therefore, we conclude that even for much longer time scales, HS is largely independent of CO_2 forcing.

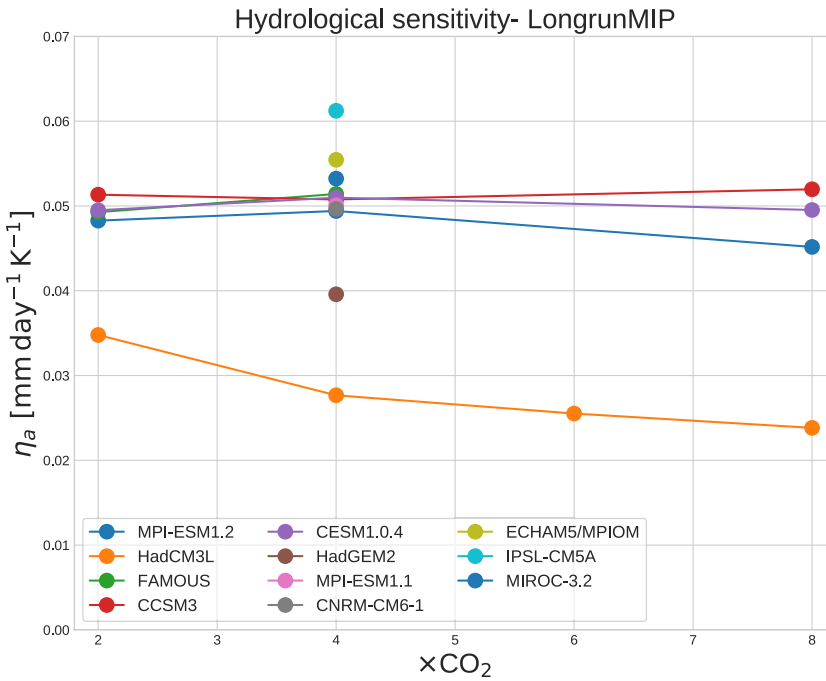

Figure 4. Apparent hydrological sensitivity parameter for abrupt ×CO_2 in LongrunMIP model runs. For 6 of these models, only the 4×CO_2 output is available.

4. Summary and Discussion

The key finding of this paper is that HS is a weak function of CO_2 forcing, especially at large concentrations. Analyzing idealized experiments with abrupt CO_2 increases in two models, we find some variations in η_a between 2× and 4×CO_2 (roughly 8% in CESM-LE, and 20% in GISS E2.1-G), but η_a becomes almost completely insensitive to the magnitude of CO_2 forcing beyond 5×CO_2. These findings are confirmed by transient 1pctCO2 experiments, with both models, and with more than 15 CMIP5 and CMIP6 models. Finally, 4 LongrunMIP models show almost no change in HS with CO_2 forcing even for long time scales.

Our findings are in good agreement with Good et al. (2012), who reported a change in HS of about 10% between 2× and 4×CO_2 in the HadCM3 model. We have confirmed their quantitative findings. However, by examining many models under different scenarios, and a much larger range of CO_2 forcing, we have reached a different conclusion, that is, that the HS is only a weak function of CO_2.

For the sake of consistency we have, up to this point, focused most of our attention on the apparent HS η_a, and only briefly discussed HS as measured by η, which can only be computed for the abrupt forcing runs. Digging a little deeper, it can be seen by contrasting panels a and b of Figure S3 in Supporting Information S1, that η shows a somewhat stronger dependence on the CO_2 forcing than η_a. However, this result appears to be model dependent: over the range 2× to 8×CO_2 η varies by 6% for the CESM-LE model but 22% for the GISS E2.1-G model. Since η and η_a are related by:

$$\eta_a = \frac{\Delta P}{\Delta T} = \frac{\eta \Delta T + A}{\Delta T} = \eta + \frac{A}{\Delta T}. \quad (2)$$

(using Equation 1 and substituting ΔP in the definition of η_a) we can use this expression to calculate η_a using η, ΔT, and A. The result of this calculation is shown in panel d of Figure S3 in Supporting Information S1 which agrees very well with η_a computed as the ratio $\Delta P/\Delta T$, in panel a. The smaller variations of η_a compared to η with CO_2 are a consequence of a compensation from the term $A/\Delta T$, as shown in panel c. This compensation explains why ECS is a strong function of CO_2 while η_a is insensitive to CO_2 forcing.

The reader may also wonder whether the key finding of our study, which pertains to the global mean precipitation, might also apply to distinct geographical regions. A very preliminary look at the model output analyzed above

reveals that HS is also a weak function of CO_2 over land, in both the abrupt and 1%/yr cases in the CESM-LE model, but a full examination of this question is beyond the scope of this short paper.

Finally, it is important to keep in mind that CO_2 is not the only forcing of the climate system. Whether other forcings are able to alter HS in a substantial way remains to be determined. Richardson et al. (2018) examined the HS in 10 models forced with carbon dioxide, methane, sulfates, aerosols, and others, and reported little difference in HS across these forcings (except for black carbon). MacIntosh et al. (2016), using the HadGEM3 model, found that ozone is able to produce a fast precipitation response. More recently, McCoy et al. (2022) suggested that the absorbing aerosols might be able to affect the HS via the fast response, similar to the findings in Richardson et al. (2018). While a careful analysis of HS changes using single forcing runs remains to be done, we have examined the largest CO_2 forcing scenarios in both CMIP5 (RCP8.5) and CMIP6 (SSP5-8.5) to determine if our key finding remains valid in a more realistic setting, that is, in the presence of other climate forcings. As shown in Figure S4 in Supporting Information S1 (List of models used is in Tables S4 and S5 in Supporting Information S1), the CMIP models show small changes in η_a in the second half of the 21st century, when the CO_2 forcing is the largest, confirming our finding. Needless to say, changes in these scenarios are difficult to interpret, as CO_2 is not the only forcing, and it is conceivable that specific forcings may be able to affect HS in specific decades, when the CO_2 forcing is not as strong. That question, however, is beyond the scope of this study.

Data Availability Statement

The CESM-LE and GISS E2.1-G data are available in a Zenodo repository at https://doi.org/10.5281/zenodo.3901624. The CMIP5 and CMIP6 data can be found on the Earth System Grid Federation (ESGF): https://esgf-node.llnl.gov/projects/esgf-llnl/. List of CMIP5 and CMIP6 models used in this paper can be found in the Supporting Information S1. LongRunMIP data is available through Rugenstein et al. (2019) and at: https://www.longrunmip.org/.

Acknowledgments

D.R. and L.M.P. are supported by a grant from the National Science Foundation to Columbia University (award number 1914569). L.M.P. and I.M. are grateful to NASA for a generous FINESST Fellowship Grant 80NSSC20K1657. A.G.P. was supported by the U.S. Department of Energy, Office of Science, Office of Biological & Environmental Research (BER), Regional and Global Model Analysis (RGMA) component of the Earth and Environmental System Modeling Program under Award Number DE-SC0022070 and National Science Foundation (NSF) IA 1947282, and by the National Center for Atmospheric Research (NCAR), which is a major facility sponsored by the NSF under Cooperative Agreement No. 1852977. Computing and data storage resources, including the Cheyenne supercomputer (https://doi.org/10.5065/D6RX99HX), were provided by the Computational and Information Systems Laboratory at NCAR. The authors also thank the high-performance computing resources provided by NASA's Advanced Supercomputing (NAS) Division and the NASA Center for Climate Simulation (NCCS). We also thank the World Climate Research Programme for collecting and archiving CMIP simulations and Maria Rugenstein and Jonah Bloch-Johnson who designed and coordinated LongRunMIP and provided the model output; we thank them as well as contributors of model simulations to the project.

References

Allen, M. R., & Ingram, W. J. (2002). Constraints on future changes in climate and the hydrologic cycle. *Nature*, *419*(6903), 228–232. https://doi.org/10.1038/nature01092

Andrews, T., Forster, P. M., Boucher, O., Bellouin, N., & Jones, A. (2010). Precipitation, radiative forcing and global temperature change. *Geophysical Research Letters*, *37*(14), L14701. https://doi.org/10.1029/2010gl043991

Bloch-Johnson, J., Rugenstein, M., Stolpe, M. B., Rohrschneider, T., Zheng, Y., & Gregory, J. M. (2021). Climate sensitivity increases under higher CO_2 levels due to feedback temperature dependence. *Geophysical Research Letters*, *48*(4), e2020GL089074. https://doi.org/10.1029/2020GL089074

Colman, R., & McAvaney, B. (2009). Climate feedbacks under a very broad range of forcing. *Geophysical Research Letters*, *36*(1), L01702. https://doi.org/10.1029/2008GL036268

Eyring, V., Bony, S., Meehl, G. A., Senior, C. A., Stevens, B., Stouffer, R. J., & Taylor, K. E. (2016). Overview of the Coupled Model Intercomparison Project Phase 6 (CMIP6) experimental design and organization. *Geoscientific Model Development*, *9*(5), 1937–1958. https://doi.org/10.5194/gmd-9-1937-2016

Fläschner, D., Mauritsen, T., & Stevens, B. (2016). Understanding the intermodel spread in global-mean hydrological sensitivity. *Journal of Climate*, *29*(2), 801–817. https://doi.org/10.1175/jcli-d-15-0351.1

Good, P., Ingram, W., Lambert, F. H., Lowe, J. A., Gregory, J. M., Webb, M. J., et al. (2012). A step-response approach for predicting and understanding non-linear precipitation changes. *Climate Dynamics*, *39*(12), 2789–2803. https://doi.org/10.1007/s00382-012-1571-1

Gregory, J. M., Andrews, T., & Good, P. (2015). The inconstancy of the transient climate response parameter under increasing CO_2. *Philosophical Transactions of the Royal Society A: Mathematical, Physical & Engineering Sciences*, *373*(2054), 20140417. https://doi.org/10.1098/rsta.2014.0417

Held, I. M., & Soden, B. J. (2006). Robust responses of the hydrological cycle to global warming. *Journal of Climate*, *19*(21), 5686–5699. https://doi.org/10.1175/jcli3990.1

Hurrell, J. W., Holland, M. M., Gent, P. R., Ghan, S., Kay, J. E., Kushner, P. J., et al. (2013). The community Earth system model: A framework for collaborative research. *Bulletin of the American Meteorological Society*, *94*(9), 1339–1360. https://doi.org/10.1175/BAMS-D-12-00121.1

Jeevanjee, N., & Romps, D. M. (2018). Mean precipitation change from a deepening troposphere. *Proceedings of the National Academy of Sciences of the United States of America*, *115*(45), 11465–11470. https://doi.org/10.1073/pnas.1720683115

Kelley, M., Schmidt, G. A., Nazarenko, L. S., Bauer, S. E., Ruedy, R., Russell, G. L., et al. (2020). GISS-e2.1: Configurations and climatology. *Journal of Advances in Modeling Earth Systems*, *12*(8), e2019MS002025. https://doi.org/10.1029/2019ms002025

MacIntosh, C., Allan, R., Baker, L., Bellouin, N., Collins, W., Mousavi, Z., & Shine, K. (2016). Contrasting fast precipitation responses to tropospheric and stratospheric ozone forcing. *Geophysical Research Letters*, *43*(3), 1263–1271. https://doi.org/10.1002/2015gl067231

McCoy, I. L., Vogt, M. A., & Wood, R. (2022). Absorbing aerosol choices influences precipitation changes across future scenarios. *Geophysical Research Letters*, *49*(8), e2022GL097717. https://doi.org/10.1029/2022GL097717

Meraner, K., Mauritsen, T., & Voigt, A. (2013). Robust increase in equilibrium climate sensitivity under global warming. *Geophysical Research Letters*, *40*(22), 5944–5948. https://doi.org/10.1002/2013GL058118

Mitevski, I., Orbe, C., Chemke, R., Nazarenko, L., & Polvani, L. M. (2021). Non-monotonic response of the climate system to abrupt CO_2 forcing. *Geophysical Research Letters*, *48*(6), e2020GL090861. https://doi.org/10.1029/2020gl090861

O'Gorman, P. A., Allan, R. P., Byrne, M. P., & Previdi, M. (2011). Energetic constraints on precipitation under climate change. *Surveys in Geophysics*, *33*(3–4), 585–608. https://doi.org/10.1007/s10712-011-9159-6

Pendergrass, A. G. (2020). The global-mean precipitation response to CO_2-induced warming in CMIP6 models. *Geophysical Research Letters*, *47*(17), e2020GL089964. https://doi.org/10.1029/2020gl089964

Richardson, T., Forster, P., Andrews, T., Boucher, O., Faluvegi, G., Fläschner, D., et al. (2018). Drivers of precipitation change: An energetic understanding. *Journal of Climate*, *31*(23), 9641–9657. https://doi.org/10.1175/jcli-d-17-0240.1

Rugenstein, M., Bloch-Johnson, J., Abe-Ouchi, A., Andrews, T., Beyerle, U., Cao, L., et al. (2019). LongRunMIP: Motivation and design for a large collection of millennial-length AOGCM simulations. *Bulletin of the American Meteorological Society*, *100*(12), 2551–2570. https://doi.org/10.1175/bams-d-19-0068.1

Taylor, K. E., Stouffer, R. J., & Meehl, G. A. (2012). An overview of CMIP5 and the experiment design. *Bulletin of the American Meteorological Society*, *93*(4), 485–498. https://doi.org/10.1175/bams-d-11-00094.1

Watanabe, M., Kamae, Y., Shiogama, H., DeAngelis, A. M., & Suzuki, K. (2018). Low clouds link equilibrium climate sensitivity to hydrological sensitivity. *Nature Climate Change*, *8*(10), 901–906. https://doi.org/10.1038/s41558-018-0272-0